Orientation of C70 molecules in peapods as a function of the nanotube diameter

Matthieu Chorro, Axel Delhey, Laure Noé, Marc Monthioux, Pascale Launois

Orientation of C_{70} molecules in peapods as a function of the nanotube diameter

Matthieu Chorro,[1] Axel Delhey,[1] Laure Noé,[2] Marc Monthioux,[2] and Pascale Launois[1,*]
[1]*Laboratoire de Physique des Solides, UMR CNRS 8502, bât. 510, Université Paris Sud, 91 405 Orsay Cedex, France*
[2]*CEMES, CNRS, 29 rue Jeanne Marvig, 31055 Toulouse Cedex 4, France*
(Received 28 June 2006; revised manuscript received 14 September 2006; published 17 January 2007)

Encapsulated C_{70} molecules packed in single-walled carbon nanotubes display different orientations depending on the nanotube radius. We present x-ray scattering data obtained on a powder of nanotubes filled with C_{70} molecules. Analytical expressions for calculating the diffraction diagram taking into account fullerene orientations are developed. The comparison between calculations and experiments allows us to conclude that the change from the lying to standing orientation—corresponding to the molecule long axis parallel and perpendicular to the tube axis, respectively—takes place when nanotubes reach a diameter of about 1.42 nm. Energy calculations are performed using a Lennard-Jones (6-12) potential, leading to a calculated reorientation diameter in good agreement with that determined experimentally.

DOI: 10.1103/PhysRevB.75.035416 PACS number(s): 61.10.Eq, 61.48.+c

I. INTRODUCTION

The observation of C_{60} fullerene molecules inside single-walled carbon nanotubes (SWNT) in 1998 (Ref. 1) led to the synthesis of new hybrid carbon nanostructures, as reviewed in Ref. 2. These nanostructures, termed peapods, are commonly described as one-dimensional periodic chains of fullerenes C_n (n=60, 70, etc.) inside the nanotubes. Nanotubes possess exceptional electronic or mechanical properties,[3,4] whose tuning by filling with fullerenes is a most interesting perspective. Indeed, modification of the local electronic structure or improvement in mechanical properties have been demonstrated for C_{60} peapods.[5,6] C_{70} peapods have been less studied than C_{60} ones up to now, but their structural and physical properties should be richer due to the ellipsoidal shape of the C_{70} fullerene as compared to the spherical one of C_{60}. Using electron diffraction, Hirahara and co-workers evidenced polymorphic packing structures in C_{70} peapods.[7] Two different orientations have been found experimentally depending on the nanotube diameter: the lying orientation where the molecule long axis is parallel to the tube axis, and the standing orientation, corresponding to molecule long axis perpendicular to the tube axis.[7–9] Interestingly, theoretical investigations point towards the dependency of electron states with the molecule orientation.[10,11]

The goal of the present work is to determine the nanotube diameter value beyond which the change from the lying to standing orientation occurs, which is not yet known precisely. The reorientation diameter is deduced from x-ray scattering measurements. An interesting property of x-ray experiments, which are made on macroscopic samples, is that contribution of out-of-statistic objects (defective nanotubes, etc.) is negligible. Analytical expressions of the scattering law taking into account molecular orientations have been developed, allowing us to simulate the measured x-ray diffractograms. The nanotube diameter distribution, distances in between fullerene centers of mass and fullerene orientations are deduced from comparison between measurements and simulations. The reorientation diameter obtained from x-ray experiments will be discussed with respect to available experimental and theoretical results in the literature. As underlined in Ref. 12, dispersion forces are notoriously difficult to determine theoretically and experimental data are needed as benchmarks guiding the choice of models. We have performed energy calculations using a Lennard-Jones (6-12) potential.[13] They allow to determine a reorientation diameter value in good agreement with that determined experimentally. It is thus shown that the Lennard-Jones potential is effective for the calculation of fullerene orientations inside nanotubes.

II. EXPERIMENT

A. Experimental part

SWNTs used in this study (Fig. 1, left-hand side) were supplied by NANOCARBLAB (Russia). They were prepared following the electric arc route (Ni+Y catalysts) then extensively purified via successive oxidation treatments including soaking in HNO_3, annealing in air and freeze drying. The purification procedure was severe enough to create openings of the SWNTs. The as-received material was disposed into a

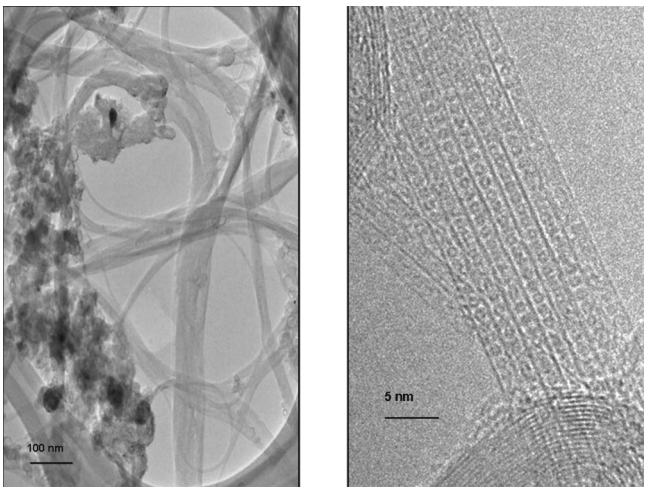

FIG. 1. (Left-hand side) Transmission electron microscopy images of SWNTs. Low magnification, SWNT bundles are shown along with empty polyaromatic carbon shells. (Right-hand side) High resolution transmission electron microscopy image of a C_{70} @SWNT peapod bundle. The resolution is not sufficient to distinguish between lying and standing C_{70} molecules.

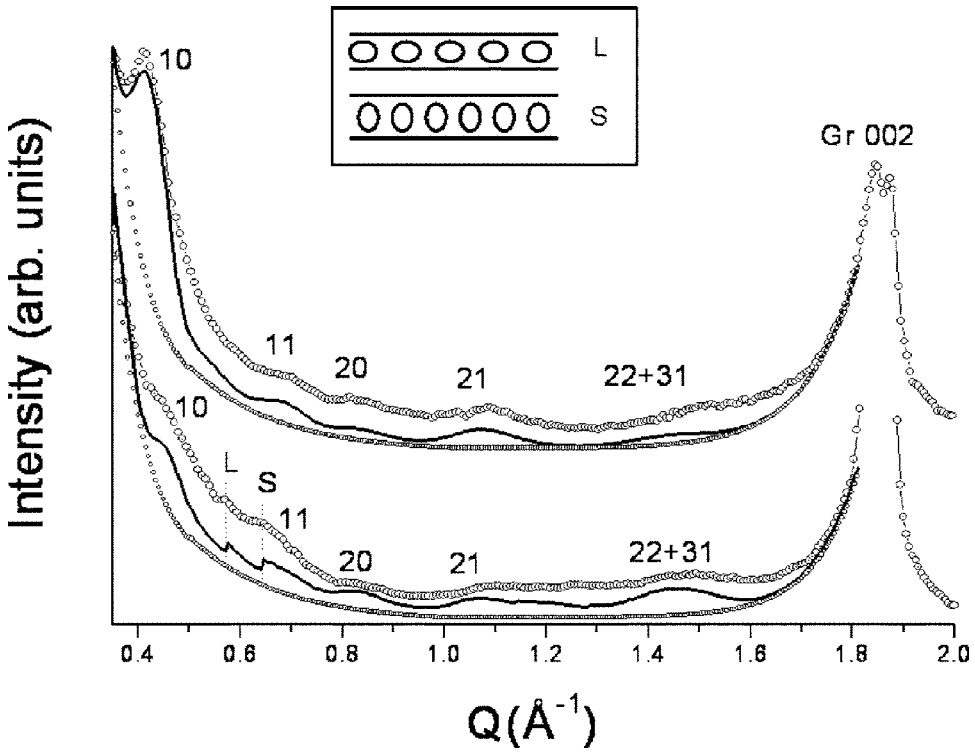

FIG. 2. Room temperature diffraction patterns of SWNTs (upper curve, open circles) and C_{70} peapods (lower curve, open circles). The curves are translated vertically for the sake of clarity. Diffuse scattering from the glass capillary—centered around 1.7 Å^{-1}—has been measured on empty capillaries and substracted to both SWNT and peapod diagrams. Below each experimental curves are represented the simulation (black thick line) and the background used for the fit (small circles). Doublets of Miller indices refer to diffraction peaks of the two-dimensional hexagonal bundle lattice. "Gr 002" refers to scattering by graphene-based impurities. The positions of the first order diffraction peaks of the periodic chains of lying and standing C_{70} molecules are indicated by the indexation *L* and *S*, respectively. Inset: representation of the lying and standing orientations for the C_{70} molecules inside nanotube.

quartz ampoule along with C_{70} powder (Alfa Aesar, more 98% pure). The amount of C_{70} was calculated so that the fullerene vapor pressure was about 1 atmosphere at the filling temperature. To outgas the whole material, the ampoule was evacuated (primary vacuum) while being heated up to 200 °C in a sand bath for 15–30 minutes then filled with argon, cycled three times. It was after heating in a tubular furnace up to 500 °C for 24 hours, to allow for the sublimation of the C_{70} powder and for the insertion of the molecules inside nanotubes. The ampoule was eventually annealed under dynamic primary vacuum up to 800 °C for 1 hour to get rid of residual (noninserted) C_{70}. From TEM images, the filling rate appears quite high (Fig. 1, right-hand side).

SWNT and C_{70} peapod powders were placed inside Lindemann glass capillaries of 1 mm diameter. Diffraction patterns were recorded in transmission on a planar imaging plate, using a rotating anode device delivering Cu $K\alpha$ wavelength ($\lambda = 1.5418$ Å) after confocal parabolic W/Si multilayer mirrors. Experiments were performed under vacuum to minimize contamination due to air scattering. Typical recording times are of about 24 hours.

B. X-ray scattering results

Diffraction patterns obtained for both SWNT and C_{70} peapod samples are shown in Fig. 2.

The first diffraction peak of the SWNT pattern is observed at wave vector $Q \simeq 0.41$ Å^{-1}, a typical value for nanotube powders produced by the electric-arc method.[14,15] Single-walled nanotubes are packed in small crystalline bundles. The peak sited at $Q \simeq 0.41$ Å^{-1} corresponds to the 10 reflection from the bidimensional hexagonal bundles lattice.[16] Higher order diffraction peaks are visible up to 1.6 Å^{-1}. The intense peaks situated around 1.85 Å^{-1} are coming from polyaromatic (graphene-based) impurities. Strong intensities at small wave vectors, below 0.4 Å^{-1}, often measured in SWNT samples, may be associated with sample porosity.

In the case of peapods, one observes a strong diminution of the intensity of the 10 peak. This peak is very sensitive to molecular encapsulation[17,18] and its diminution allows one to estimate the filling rate of the nanotubes by the C_{70} molecules. The higher order diffraction peaks from the bundle lattices are clearly visible between 0.8 and 1.6 Å^{-1}, showing that the filled nanotubes are still well crystallized in hexagonal bundles. Two additional peaks, at wave-vector values $Q \simeq 0.57$ Å^{-1} and 0.63 Å^{-1}, are also present. A similar result was obtained in a previous x-ray diffraction study performed by Maniwa and co-workers on peapods made from SWNTs synthesized by the laser ablation method.[19] Following the well-known relation $Q = 2\pi/L$, the two additional diffraction peaks are found to correspond to distances $L \simeq 11$ Å $= 1.1$ nm and 10 Å $= 1$ nm in direct space, respectively. The C_{70} molecule has an ellipsoidal shape with short and long

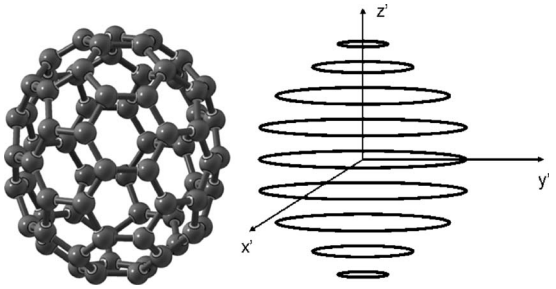

FIG. 3. The C_{70} molecule: atomic model and homogeneous approximation.

axes, respectively, equal to about 0.71 and 0.81 nm. The measured distances roughly correspond to distances in between two lying molecules or two standing ones when the van der Waals distance ($\simeq$0.3 nm) between them is taken into account.[7,19] The two additional diffraction peaks observed for C_{70} peapod sample can thus be attributed to periodic linear arrangements of lying and of standing molecules inside the nanotubes.

III. ANALYTICAL EXPRESSIONS FOR THE SCATTERING LAW

An analytic formula is built up to calculate the scattered intensity of a C_{70} peapod powder. Analytical descriptions of the diffraction pattern of C_{60} peapods have been given in Ref. 18. Diffraction by C_{70} peapods is more difficult to calculate due to orientational effects. The range of investigated wave vectors being smaller than 2 $Å^{-1}$, homogeneous approximation can be used. We modelize the C_{70} fullerene as formed of nine circles ν of height ξ_ν and radius $R_{\nu\perp}$ (see Fig. 3 and Table I).

A. The C_{70} form factor in lying and standing orientations

The molecule form factor can be first calculated in the system (R') of the C_{70} molecule, where the z' axis is the molecule long axis, and then in the system (R) of the nanotube, where the Z axis is the tube axis. The cylindrical coordinates of the wave vector $\vec{Q}$ are $(Q'_z, Q'_\perp, \varphi'_{\vec{Q}})$ in (R') and $(Q_z, Q_\perp, \varphi_{\vec{Q}})$ in (R), as is illustrated in Fig. 4. The form factor is the Fourier transform of the molecule electronic density. In the molecule system (R'), it thus writes

$$F_{C_{70}}(\vec{Q}) = f_c(Q)\sum_{\nu=0}^{8} n_\nu R_{\nu\perp} \exp(iQ'_z\xi_\nu) \times \int_0^{2\pi} \exp[iQ'_\perp R_{\nu\perp}\cos(\varphi_\nu - \varphi'_{\vec{Q}})]d\varphi_\nu.$$

Integration is performed over each atomic circle ν (see Figs. 3 and 4, and Table I). φ_ν is the polar angle of a point M over the circle ν, $R_{\nu\perp}$ the radius of circle ν, ξ_ν is its z' coordinate and n_ν is the linear atomic density along the circle. $f_c(Q)$ is the scattering form factor of a carbon atom. It follows that

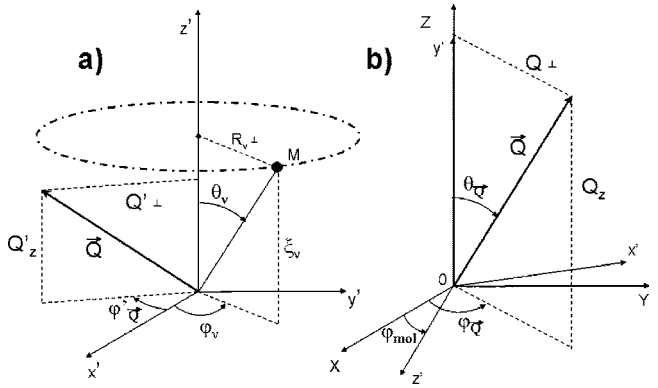

FIG. 4. Representation of the coordinates used in the calculation: (a) in the molecule system $(R'=0x'y'z')$ and (b) in the nanotube system $(R=0XYZ)$. In (b), the orientation of the molecular long axis $0z'$ and of the molecule system of coordinates $(0x'y'z')$ in the standing case is drawn.

$$F_{C_{70}}(\vec{Q}) = f_c(Q)\left(N_0 J_0(Q'_\perp R_{0\perp}) + 2\sum_{\nu=1}^{4} N_\nu \cos(Q'_z\xi_\nu) J_0(Q'_\perp R_{\nu\perp})\right), \quad (1)$$

N_ν being the number of carbon atoms on circle ν and J_0 the cylindrical Bessel function of order zero $\{J_0(x) = \frac{1}{2\pi}\int_0^{2\pi} \exp[ix\sin(t)]dt\}$. The systems of coordinates (R) and (R') coincide for the lying molecule, and one thus directly obtains the lying form factor in (R) as

$$F_{C_{70}\text{Lying}}(Q, Q_z) = f_c(Q)\left(N_0 J_0(\sqrt{Q^2 - Q_z^2}R_{0\perp}) + 2\sum_{\nu=1}^{4} N_\nu \cos(Q_z\xi_\nu) J_0(\sqrt{Q^2 - Q_z^2}R_{\nu\perp})\right). \quad (2)$$

For the standing case, the molecule long axis is in the plane

TABLE I. The C_{70} molecule characteristics within homogeneous approximation. The index ν label the circles, ξ_ν and $R_{\nu\perp}$ refer to their coordinate along the molecule long axis and to their radii, respectively. N_ν is the number of carbon atom and n_ν is the linear atomic density.

ν	ξ_ν (nm)	$R_{\nu\perp}$ (nm)	N_ν	n_ν (atom/Å)
0	0	0.3565	10	0.446
1	0.1197	0.3461	10	0.460
2	0.2449	0.3005	10	0.529
3	0.3235	0.2401	5	0.331
4	0.3983	0.1243	5	0.640
5	−0.1197	0.3461	10	0.460
6	−0.2449	0.3005	10	0.529
7	−0.3235	0.2401	5	0.331
8	−0.3983	0.1243	5	0.640

$(0xy)$, making the angle φ_{mol} with $0x$ (Fig. 4). Using relations between coordinates of the wave vector $\vec{Q}$ in the systems (R) and (R'), one obtains for the standing form factor in (R),

$$F_{\mathrm{C_{70}Standing}}(Q,Q_z,\varphi_{\mathrm{mol}}) = f_c(Q)\Bigg(N_0 J_0[\sqrt{Q^2\sin^2(\varphi_{\vec{Q}}-\varphi_{\mathrm{mol}})+Q_z^2\cos^2(\varphi_{\vec{Q}}-\varphi_{\mathrm{mol}})}R_{0\perp}] + 2\sum_{\nu=1}^{4} N_\nu \cos[\sqrt{Q^2-Q_z^2}\cos(\varphi_{\vec{Q}}-\varphi_{\mathrm{mol}})\xi_\nu] J_0[\sqrt{Q^2\sin^2(\varphi_{\vec{Q}}-\varphi_{\mathrm{mol}})+Q_z^2\cos^2(\varphi_{\vec{Q}}-\varphi_{\mathrm{mol}})}R_{\nu\perp}]\Bigg). \tag{3}$$

B. Scattered intensity from a powder of C_{70} peapods: analytical formula

Let us consider nanotubes with diameter Φ_T, their length being assumed to be infinite (the infinite length hypothesis means that nanotube length is large when compared to experimental resolution). Nanotubes are assembled into hexagonal bundles. The nanotube filling rate by fullerenes is p $(0 \leqslant p \leqslant 1)$. Fullerenes are assumed to form long chains (longer than resolution) inside the nanotubes, which means that the formula derived here should not be used for very small filling rates. Detailed demonstration of the scattered intensity formula is developed in the lying case; it could be easily done by the reader, using the same approach, in the standing case. Spherical approximation will eventually be discussed for comparison.

In the *lying case*, the form factor of a peapod of length L, containing one C_{70} molecule at half-height, writes

$$F(\vec{Q}) = a_T J_0\left(\frac{Q_\perp \Phi_T}{2}\right)\frac{\sin(Q_z L/2)}{Q_z L/2} + F_{\mathrm{C_{70}Lying}}(\vec{Q}),$$

where $a_T = f_c(Q)\pi\Phi_T L\sigma_T$. f_c is the carbon form factor, σ_T is the density of carbon atoms on the nanotube ($\sigma_T \simeq 0.37$ atom/Å^2), Q_z and $Q_\perp$ are the components of the wave vector $\vec{Q}$ along the tube axis and perpendicular to it, Q is its modulus. The form factor is the sum of two terms: a nanotube term and a fullerene term. For a bundle of peapods of length $N_c L$, one obtains

$$F(\vec{Q}) = \sum_i \left[a_T J_0\left(\frac{Q_\perp \Phi_T}{2}\right)\frac{\sin(Q_z L/2)}{Q_z L/2} + F_{\mathrm{C_{70}Lying}}(\vec{Q})\exp[iQ_z T_z(i)]\right]\exp(i\vec{Q}_\perp \vec{R}_i) \times \sum_{n=0}^{N_c-1}\exp(iQ_z nL), \tag{4}$$

where $\vec{R}_i$ is the position of tube i perpendicularly to the bundle axis and $T_z(i)$ is the position of a molecule of the chain i along the $0z$ axis of the nanotube. It will be assumed that there are no correlations in z positions for molecular chains in different tubes, as discussed theoretically in Ref. 20. Intensity per length unit writes

$$I(\vec{Q}) = \sum_{i,j}\left[a_T J_0\left(\frac{Q_\perp \Phi_T}{2}\right)\frac{\sin(Q_z L/2)}{Q_z L/2} + F_{\mathrm{C_{70}Lying}}(\vec{Q})\exp[iQ_z T_z(i)]\right] \times \left[a_T J_0\left(\frac{Q_\perp \Phi_T}{2}\right)\frac{\sin(Q_z L/2)}{Q_z L/2} + F_{\mathrm{C_{70}Lying}}(\vec{Q})\exp[-iQ_z T_z(j)]\right]\exp[i\vec{Q}_\perp(\vec{R}_i-\vec{R}_j)]\frac{1}{N_c L} \times \sum_{n,m=0}^{N_c-1}\exp[iQ_z(n-m)L]. \tag{5}$$

Using the relation

$$\lim_{N_c\to\infty}\frac{1}{N_c L}\sum_{n,m=0}^{N_c-1}\exp[iQ_z(n-m)L] = \frac{2\pi}{L^2}\sum_{k=-\infty}^{\infty}\delta(Q_z - 2\pi k/L),$$

where $\delta(x)$ is the Dirac distribution and where k, n, and m are integers, and averaging over the random variables $T_z(i)$, one then gets, for parallel bundles of infinite tubes filled with infinite chains of C_{70} molecules separated by distance L,

$$I_{\mathrm{Lying}}(\vec{Q}) = \frac{2\pi}{L^2}\Bigg\{\sum_{i,j}\exp[i\vec{Q}_\perp(\vec{R}_i-\vec{R}_j)] \times \left[a_T J_0\left(\frac{Q_\perp \Phi_T}{2}\right) + F_{\mathrm{C_{70}Lying}}(\vec{Q})\right]^2\delta(Q_z) + N_f\sum_{k=-\infty,k\neq 0}^{\infty} F_{\mathrm{C_{70}Lying}}(\vec{Q})^2\delta(Q_z - k2\pi/L)\Bigg\}, \tag{6}$$

N_f is the total number of tubes per bundle. The $\delta(Q_z)$ dependent term is the Fourier transform of the atomic density projected on a plane perpendicular to the nanotube axis, while the $\delta(Q_z - k2\pi/L)$ dependent term comes from the periodicity of the C_{70} chain. Note that in principle, the fullerene

chain should not be considered as a one-dimensional (1D) crystal but as a 1D liquid. The rigorous treatment is given in Refs. 21 and 22 for a C_{60} chain. However, peak widths are found to be extremely narrow, which validates the crystalline approach.

If the filling rate p is not equal to 1, with still long chains of molecules, Eq. (6) becomes

$$I_{\mathrm{Lying}}(\vec{Q}) = \frac{2\pi}{L^2}\left\{ \sum_{i,j} \exp[i\vec{Q}_{\perp}(\vec{R}_i - \vec{R}_j)] \times \left[a_T J_0\left(\frac{Q_{\perp}\Phi_T}{2}\right) + pF_{\mathrm{C_{70}Lying}}(\vec{Q}) \right]^2 \delta(Q_z) + N_f \sum_{k=-\infty, k\neq 0}^{\infty} p^2 F_{\mathrm{C_{70}Lying}}(\vec{Q})^2 \delta(Q_z - 2\pi k/L) \right\}. \tag{7}$$

To obtain now the scattered intensity from a powder of peapods, one must average intensities over all orientations of the wave vector $\vec{Q}$,

$$I_{p,\mathrm{Lying}}(Q) = \frac{1}{4\pi}\int_0^{\pi} d\theta_{\vec{Q}} \sin(\theta_{\vec{Q}}) \int_0^{2\pi} d\varphi_{\vec{Q}} I_{\mathrm{Lying}}(\vec{Q}) \tag{8}$$

Note that $\int_0^{\pi} g(Q,Q_z)\delta(Q_z - k2\pi/L)\sin(\theta_{\vec{Q}})d\theta_{\vec{Q}} = \frac{1}{Q}\int_{-1}^{1} g(Q,Qu)\delta(u - k\frac{2\pi}{QL})du = \frac{1}{Q}g(Q,k\frac{2\pi}{L})$ if $-1 \leqslant k\frac{2\pi}{QL} \leqslant 1$ and 0 if not. Combining Eqs. (6) and (8), one obtains the expression of the scattered intensity for a powder of peapods of lying C_{70} molecules,

$$I_{p,\mathrm{Lying}}(Q) = \frac{\pi}{QL^2}\left\{ \sum_{i,j} J_0(QR_{ij}) \times \left[a_T J_0\left(\frac{Q\Phi_T}{2}\right) + pF_{\mathrm{C_{70}Lying}}(Q, Q_z = 0) \right]^2 + 2N_f \sum_{k=1}^{\mathrm{Int}(QL/2\pi)} p^2 F_{\mathrm{C_{70}Lying}}\left(Q, Q_z = k\frac{2\pi}{QL}\right)^2 \right\} \tag{9}$$

$\mathrm{Int}(\frac{QL}{2\pi})$ is the integer part of $\frac{QL}{2\pi}$ and R_{ij} is the modulus of the vector $(\vec{R}_i - \vec{R}_j)$. Note that if there are no fullerenes (C_{70} form factor taken equal to zero), one finds the already-known expression for the scattered intensity by a powder of SWNT bundles (see Ref. 15 or Chap. 3 in Ref. 4),

$$I_{p,\mathrm{NT}}(Q) = \frac{\pi}{Q}\left[\pi f_c(Q)\Phi_T\sigma_T J_0\left(\frac{Q\Phi_T}{2}\right)\right]^2 \sum_{i,j} J_0(QR_{ij}). \tag{10}$$

Let us now consider the *standing case*. It can be assumed that standing molecules present all possible orientations of their long axis in the plane perpendicular to the tube axis at room temperature (see energy calculations in Sec. V). Following the approach developed in the lying case, the scattered intensity for a powder of peapods of standing molecules is found to write

$$I_{p,\mathrm{Standing}}(\vec{Q}) = \frac{\pi}{QL^2}\left\{ \sum_{i,j} J_0(QR_{ij})\left[a_T J_0\left(\frac{Q\Phi_T}{2}\right) + p\langle F_{\mathrm{C_{70}Standing}}(Q, Qz = 0)\rangle \right]^2 + N_f \sum_{k=-\infty, k\neq 0}^{\infty} p^2 \langle F_{\mathrm{C_{70}Standing}}(Q, Q_z = k2\pi/L)\rangle^2 \right\} + \frac{N_f}{4\pi L}\int_0^{\pi} d\theta_{\vec{Q}} \sin(\theta_{\vec{Q}}) \int_0^{2\pi} d\varphi_{\vec{Q}} [\langle F_{\mathrm{C_{70}Standing}}(\vec{Q})^2\rangle - \langle F_{\mathrm{C_{70}Standing}}(\vec{Q})\rangle^2]. \tag{11}$$

The mean values are taken over the orientation angle φ_{mol} of the molecule long axis in the plane perpendicular to the nanotube axis. The last term in this equation is a Laue term characteristic of random orientational disorder.[23] In the Q range of interest ($Q \leqslant 2$ Å^{-1}), the Laue-type term is calculated to be negligible compared to the first two terms of the equation. Orientational disorder between standing molecules can hardly be detected from powder diffraction patterns. Calculation of the diffraction pattern assuming that standing molecules have the same orientation within one tube but different orientations in different tubes (not detailed here) give almost the same diagram as Eq. (11).

A last case can be considered for the sake of comparison: the C_{70} molecule can be approximated by homogeneous *spherical shells*.[19] In such a case, the C_{70} form factor simply writes

$$F_{\mathrm{C_{70}Sph}}(Q) = f_c(Q)\sum_{\nu=0}^{4} N'_{\nu}\frac{\sin(QR_{\nu})}{QR_{\nu}},$$

where, with respect to Table I, $R_{\nu} = \sqrt{R_{\nu\perp}^2 + \xi_{\nu}^2}$, $N'_0 = N_0$, and $N'_{\nu} = 2N_{\nu}$ for $\nu = 1-4$. The intensity scattered by a powder of peapods (filling rate p) can be calculated using the same formalism as for spherical C_{60} molecules (Ref. 18). It writes

$$I_{p,\mathrm{Sph}}(Q) = \frac{\pi}{QL^2}\left\{ \sum_{i,j} J_0(QR_{ij})\left[a_T J_0\left(\frac{Q\Phi_T}{2}\right) + pF_{\mathrm{C_{70}Sph}}(Q)\right]^2 + 2N_f\,\mathrm{Int}\left(\frac{QL}{2\pi}\right)p^2 F_{\mathrm{C_{70}Sph}}(Q)^2 \right\}. \tag{12}$$

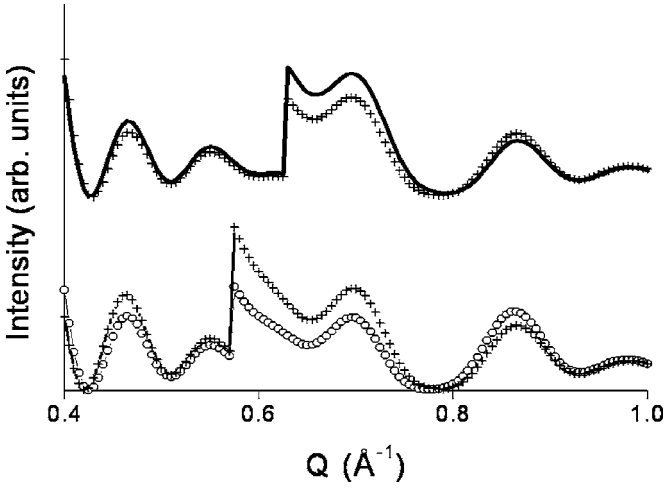

FIG. 5. Scattered intensity calculated: up, for standing (line) and spherical (crosses) C_{70} molecules inside nanotubes, the interfullerenes distance being $L=1$ nm; down, for lying (open circles) and spherical (crosses) molecules with $L=1.1$ nm. L values are taken from experiments (Sec. II B). Other parameters are $\Phi_T=1.4$ nm, $N_f=19$, $p=1$.

C. Discussion

Diffraction patterns for powders of nanotubes filled with either standing or lying molecules and with molecules approximated as concentric spherical shells are drawn in Fig. 5. Significant changes in intensities are evidenced when the standing or lying cases are compared with the spherical one at $Q=2\pi/L$, L being the period of the one-dimensional molecular chain. In Ref. 19, which, to our knowledge, gives the only report before this paper for x-ray scattering on C_{70} peapods, analysis was performed approximating the C_{70} molecule to homogeneous spherical shells. Figure 5 shows that the use of the homogeneous spherical shell approximation to analyze given experimental data leads to an overestimate of the proportion of standing molecules and to an underestimate of the lying molecules. It is thus important to take into account the molecule orientations to analyze the experimental diffraction patterns. Such analysis is presented in Sec. IV B.

IV. SIMULATION OF X-RAY SCATTERING RESULTS

A. Nanotubes

As discussed by Rols and co-workers,[15] detailed analysis of x-ray diffraction patterns from SWNT powders allows one to determine the structural characteristics of the nanotubes, namely the tube diameters and the average number of nanotubes within a bundle. SWNT powders consist of nanotubes having the same diameter within one bundle but with a distribution of tube diameters between different bundles. For such a powder, the calculated intensity writes

$$I^{\mathrm{NT}}(Q)=\int_0^\infty d\Phi_T p(\Phi_T) I_{p,\mathrm{NT}}^{\Phi_T}(Q), \tag{13}$$

where $p(\Phi_T)$ is the normalized distribution of diameters and where $I_{p,\mathrm{NT}}^{\Phi_T}(Q)$ is the intensity of a powder of identical bundles of nanotubes of diameter Φ_T, given in Eq. (10). For comparison with experiments, one should in principle consider absorption, polarization, and geometrical correction factors, convolution by the resolution function, together with the addition of a background function. In the present case, absorption and resolution effects are neglected (the Q dependence of the absorption correction factor is calculated to be very small and the resolution function is narrow, with full-width at half-maximum FWHM=0.02 Å^{-1}). The simulated intensity, which can be directly compared to experimental data, thus writes

$$I_{\mathrm{sim}}^{\mathrm{NT}}(Q)=\alpha I^{\mathrm{NT}}(Q)p(Q)g(Q)+\mathrm{BG}(Q), \tag{14}$$

α is an adjustable scaling coefficient. $p(Q)=\frac{1+cos^2(2\theta_B)}{2}$ {with $\theta_B=\mathrm{asin}[\lambda Q/(4\pi)]$} is the polarization factor. This formula is established for unpolarized x rays: corrections due to polarization by the multilayer mirrors can be neglected because their reflection angle ($\simeq 1.5°$) is small enough. $g(Q)=\cos^3(2\theta_B)$ is the geometrical correction factor for a planar detector. The background function $\mathrm{BG}(Q)$ has been adjusted to account for low wave-vector intensity due to sample porosity and to contamination by graphitic impurities around 1.85 Å^{-1}.

As is shown in Fig. 2, a very good agreement between the experimental diffraction pattern and the simulated one is obtained for $N_T=19$ tubes per bundle and for a Gaussian distribution in tube diameters: the mean tube diameter value is 1.42 nm and the distribution width FWHM is 0.2 nm. The distribution of nanotube diameters in the reference sample being determined, one can now focus on peapods.

B. Peapods

To analyze the diffraction patterns of C_{70} peapods, one defines two critical nanotube diameters: (i) the minimum diameter Φ_{enc} allowing the fullerene encapsulation, and (ii) the diameter Φ_{LS} corresponding to the change from the lying to the standing orientation. Molecules inside nanotubes of diameters smaller than Φ_{LS} are assumed to have the lying orientation and molecules in nanotubes of larger diameters have standing orientation. The calculated intensity writes

$$\begin{aligned} I^{\mathrm{peapods}}(Q)=&\int_0^{\Phi_{\mathrm{enc}}} d\Phi_T p(\Phi_T) I_{p,\mathrm{NT}}^{\Phi_T}(Q) \\ &+\int_{\Phi_{\mathrm{enc}}}^{\Phi_{LS}} d\Phi_T p(\Phi_T) I_{p,\mathrm{Lying}}^{\Phi_T}(Q) \\ &+\int_{\Phi_{LS}}^{\infty} d\Phi_T p(\Phi_T) I_{p,\mathrm{Standing}}^{\Phi_T}(Q). \end{aligned} \tag{15}$$

The nanotube diameter distribution function $p(\Phi_T)$ is determined on the reference nanotube powder; $I_{p,\mathrm{NT}}^{\Phi_T}(Q)$, $I_{p,\mathrm{Lying}}^{\Phi_T}(Q)$, and $I_{p,\mathrm{Standing}}^{\Phi_T}(Q)$ are the calculated intensities from powders of nanotubes, peapods with lying molecules and peapods with standing molecules, respectively, for nanotubes with diameter Φ_T [Eqs. (10), (9), and (11)]. Comparing the simulated intensity

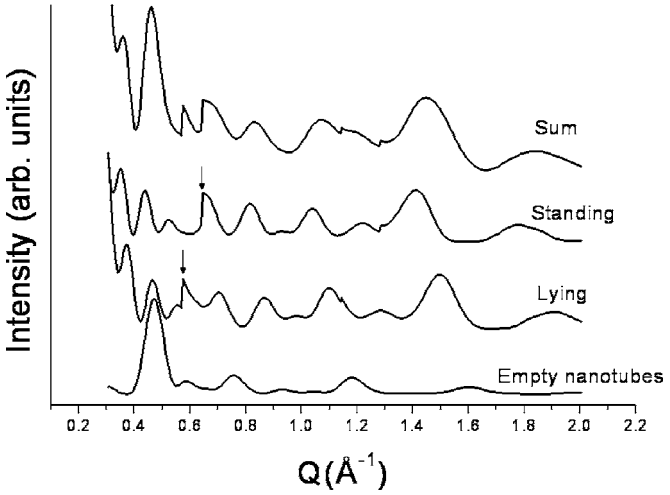

FIG. 6. The three components of the intensity and their sum. They have been translated vertically for the sake of clarity; the background function BG(Q) is not taken into account here. Arrows point toward the diffraction peaks from chains of lying or standing molecules.

$$I_{\text{sim}}^{\text{peapods}}(Q) = \alpha I^{\text{peapods}}(Q)p(Q)g(Q) + \text{BG}(Q) \qquad (16)$$

with the measured data, one obtains the best agreement between measured and simulated patterns (Fig. 2) for $\Phi_{\text{enc}} = 1.32$ nm and $\Phi_{LS} = 1.42$ nm. Uncertainties are estimated to be of 0.02 nm. Indeed, agreement between simulation and experiment is still correct for $\Phi_{\text{enc}} \pm 0.02$ nm or $\Phi_{LS} \pm 0.02$ nm, while it is worse for $\Phi_{\text{enc}} \pm 0.04$ nm or $\Phi_{LS} \pm 0.04$ nm. The interfullerene distance is determined as 1.1 nm for lying molecules and 0.98 nm for standing ones. The filling rate p is found to be about 90% for peapods with both lying and standing molecules. It might be noted that agreement between simulations and experiments, although evidential, is not as good as for empty nanotubes. Clues for improving it will be discussed in Sec. V D.

As stated in Eq. (15), the simulated diffraction pattern in Fig. 2 is the sum of three components, which are drawn separately in Fig. 6 to allow the reader to visualize the different contributions to the diffraction pattern. The first one corresponds to the intensity coming from empty nanotube bundles (Φ_T smaller than 1.32 nm) and gives a relatively intense 10 Bragg peak. The second component corresponds to diameters greater than 1.32 nm and smaller than 1.42 nm: the fullerenes inside the tubes have the lying orientation, with a center-to-center distance equal to 1.1 nm. Finally, for diameters greater than 1.42 nm, intensity comes from peapods made of standing C_{70} fullerenes with interfullerene distance of about 0.98 nm.

C. Discussion

The interfullerene distances of 0.98 and 1.1 nm deduced from our x-ray measurements are in good agreement with results obtained by other authors for C_{70} peapods.[7,19] Note also that the period of 0.98 nm for the chain of standing C_{70} molecules is in good agreement with results obtained on C_{60} chains. The period is the same for C_{60} chains (see Refs. 7, 18, 19, and 24). Accordingly the diameter of ellipsoidal C_{70} along its short axes, which correspond to the stacking direction in chains of standing molecules, is very close to that of spherical C_{60}.

The nanotube diameter corresponding to the change between lying and standing orientations is found to be $\Phi_{LS} = 1.42 \pm 0.02$ nm. Other authors[8,9] concluded, from Raman scattering and high-resolution electron spectroscopy, that 1.36 nm nanotubes are filled with lying C_{70} molecules and that 1.49 nm nanotubes are filled with standing molecules. These results are in agreement with those deduced from x-ray experiments, but we emphasize that the present paper reports the accurate determination of the frontier between lying and standing orientations.

TABLE II. Lennard-Jones constants in graphitic systems, from Ref. 13.

	A (eV Å^6)	B (eV Å^{12})
Fullerene-fullerene	20.0	$34.8 * 10^3$
Tube-fullerene	17.4	$29.0 * 10^3$

V. ENERGY CALCULATIONS

Organization of fullerenes inside nanotubes has been discussed theoretically using several approaches: energy calculations with a simple van der Waals model[12,13,25] or a modified one,[21,22] annealing, Monte Carlo or molecular dynamics methods,[20,26,27] and eventually total-energy electronic-structure calculations or density-functional based tight-binding calculations.[8,10,11] The last references address the question of the orientations of the C_{70} molecules. Here, we approach this question using a van der Waals model. An overview of modified van der Waals models which have been developed for fullerenes is presented in Ref. 28 illustrating the difficulty to describe correctly all physical properties of fullerenes; in this paper, we have chosen to focus on the simplest model.[13] Our results will be compared with those of total-energy electronic-structure calculations in Sec. V D.

The Lennard-Jones potential for two atoms at distance x apart is

$$u(x) = -\frac{A}{x^6} + \frac{B}{x^{12}}. \qquad (17)$$

Following Girifalco and co-workers,[13] slightly different values of the constants A and B will be considered depending on the fact that the carbon atoms in interaction belong to two fullerenes or to a fullerene and a nanotube (Table II). The nanotube is considered as an infinite cylinder with homogeneous surface density $\sigma_T = 0.37$ atom/Å^2. The fullerene is described, like in the diffraction model, as formed of nine homogeneous circles with linear densities n_ν (see Table I). The energy of interaction between two C_{70} molecules is

$$E_{\text{full-full}} = \sum_{\nu,\mu=0}^{8} n_\nu n_\mu \int u(x) dl_{1,\nu} dl_{2,\mu}, \qquad (18)$$

where x is the distance between the two linear elements $dl_{1,\nu}$ and $dl_{2,\mu}$ on circles ν and μ of the interacting molecules 1

and 2. The nanotube-fullerene interaction writes similarly

$$E_{\text{tube-full}} = \sigma_T \sum_{\nu=0}^{8} n_\nu \int u(x) dl_\nu d\Sigma, \tag{19}$$

where x is the distance between the linear element dl_ν on the molecule and the surface element $d\Sigma$ on the nanotube. More details are given in the Appendix.

In nanotubes with large diameters, fullerenes can form zigzag or helix structures,[20,26] while in nanotubes with smaller diameters, they form linear chains. We consider here the case of linear chains. Due to the rapid decrease of van der Waals interactions with distance, one can neglect the second neighbor interactions between fullerenes, interactions between fullerenes in different tubes of a bundle or between fullerenes in a tube with the adjacent tube. The total energy per molecule of the peapod then simply writes

$$E_{\text{tot}} = E_{\text{full-full}} + E_{\text{full-tube}}. \tag{20}$$

Let us discuss below each term of this equality for lying or for standing molecules.

A. The fullerene-fullerene energy

Two different cases are considered: (i) the lying case where the only parameter in energy calculations is the distance L in between the molecule centers, (ii) the standing case in which there is a supplementary degree of freedom: the angle ψ between the molecule long axes viewed in the (XY) plane. The ψ dependence of the energy is found to be weak. It is of about 0.015 eV for $L=0.96$ nm and of only 0.005 eV for $L=1.01$ nm. For small distances such as $L \simeq 0.96$ nm, energy minima in ψ correspond to molecules rotated by 90° while they correspond to parallel molecules for $L \simeq 1.01$ nm with intermediate orientations between. Indeed, for small distances, the repulsive part of the Lennard-Jones interaction is important and the molecules minimize their looking parts by rotating one with respect to the other, while attraction makes them parallel for larger distances. Whatever it is, the small differences in energy as a function of ψ mean that at room temperature molecules will more or less present all orientations in ψ (300 K $\simeq$ 0.026 eV $\gg$ 0.005 eV). The energy of interaction $E_{\text{full-full}}$ is shown as a function of L in Fig. 7. The minimum in energy gives the equilibrium configuration for a chain of molecules. For a chain of lying molecules, the equilibrium distance is $L=1.13$ nm and for a chain of standing molecules, equilibrium corresponds to $L=1.01$ nm and $\psi=0$. Energy per molecule of a chain of standing molecules (−0.36 eV) is smaller than that of a chain of lying molecules (−0.26 eV). Molecules in an isolated chain would thus take the standing orientation with respect to the chain axis rather than the lying one.

B. The tube-fullerene energy

The interaction energy between a C_{70} molecule inside a nanotube and the nanotube is drawn in Fig. 8 for a molecule in lying or in standing orientation. In the calculations, molecule position was fixed on the central axis of the nanotube.

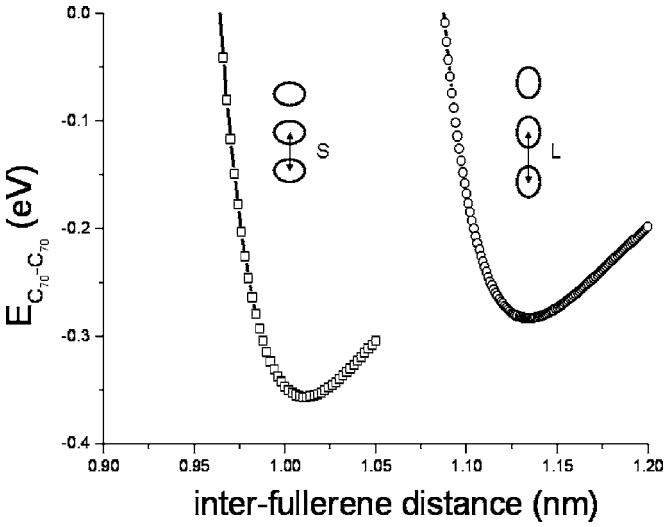

FIG. 7. Interaction between two C_{70} molecules as a function of the distance L between their centers. Open squares correspond to parallel standing molecules and open circles to lying molecules.

The interaction energy $E_{\text{tube-full}}$ is named entrance potential in Ref. 13 or reaction energy for fullerene encapsulation in Refs. 10 and 11. It can be defined by the following process:

$$C_{70} + \text{nanotube} \rightarrow C_{70}@\text{nanotube} + E_{\text{tube-full}}.$$

One deduces from Fig. 8 that the minimum nanotube diameter for the insertion of a C_{70} molecule, corresponding to $E_{\text{tube-full}}=0$, is about 1.26 nm. It can also be shown in Fig. 8 that a molecule adopts the lying orientation in thin tubes and the standing one in thick tubes (a similar result is obtained in Ref. 11; it is a rather obvious result which can be deduced from simple steric hindrance considerations). For a single molecule inside the tube, the critical tube diameter between lying and standing orientations, corresponding to the intersection between the energy curves of lying and standing molecules, is found to be $\Phi_{LS} \simeq 1.45$ nm.

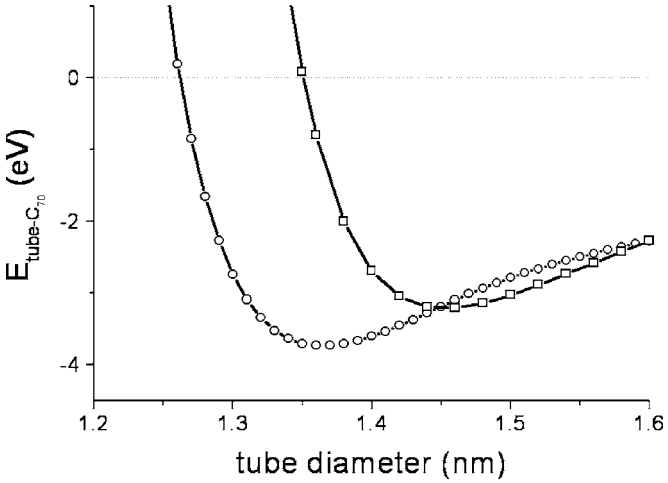

FIG. 8. Energy of a C_{70} molecule inside a nanotube as a function of the tube diameter (open circle, lying molecule; open square, standing one).

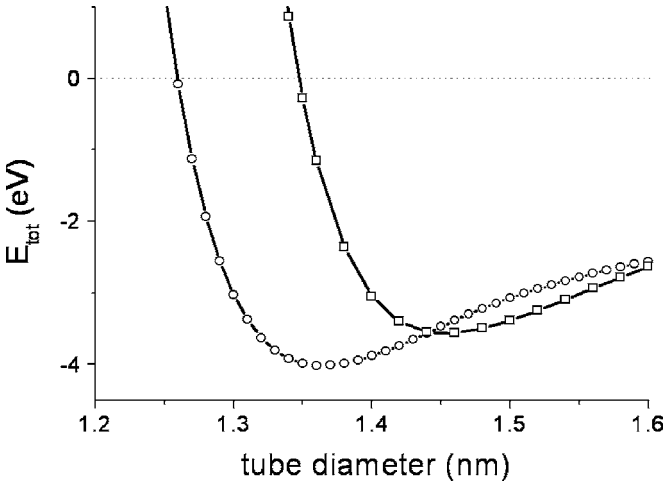

FIG. 9. Total energy per molecule in the lying case (open circles) and in the standing case (open squares, $\psi=0$).

C. The total energy

The total energy per molecule in the peapod, which is the sum of the fullerene-fullerene and fullerene-tube energies, is shown in Fig. 9. The interaction energy between two molecules being lower in the standing case than in the lying case, the critical diameter Φ_{LS} between lying and standing orientations is slightly displaced towards lower values with respect to the one determined above for isolated molecules. It is found to be $\Phi_{LS}=1.44$ nm.

D. Discussion

Let us first discuss the results of our calculation with respect to experiments. The critical diameter Φ_{LS} between lying and standing orientations is determined to be 1.44 nm from our calculations and 1.42 ± 0.02 nm from x-ray diffraction experiments. Good agreement is thus obtained here. It should however be noticed that the agreement is not as good as far as interfullerene distances are concerned: calculations give $L=1.01$ and 1.13 nm for standing and lying molecules, respectively, while experiments give $L=0.98$ and 1.1 nm. Calculations lead to a slight overestimate of the interfullerene distances. As for the value of the entrance diameter Φ_{ent}, different values are deduced from calculations and experiments: the calculated diameter is 1.26 nm while the diameter deduced from x-ray measurements is 1.32 ± 0.02 nm. But one should underline that the energetic model does not take into account the temperature while fullerene encapsulation is carried out at about 600 °C. Differences in entropy between fullerenes inside and outside the tubes should thus be taken into account. The entropy being higher outside the nanotube than inside the tube, insertion will not occur for the diameter corresponding to $E_{\text{tube,full}}=0$ but for larger diameters ($E_{\text{tube,full}}=-T\Delta S$ where T is the temperature of encapsulation and ΔS is the difference in entropy between a free and an encapsulated molecule). This may explain why the value of Φ_{ent} deduced from energy calculations is smaller than the measured one.

We now compare in Tables III and IV calculations performed within the scope of a van der Waals (vdW) model with total-energy electronic-structure (TEES) calculations in Ref. 11 (from Table I and Fig. 2 in this paper). Interfullerene distances (Table III) appear to be better evaluated using TEES calculations (with calculated values of 0.99 and 1.11 nm, as compared to the experimental ones of about 0.98 and 1.1 nm). Interaction energies obtained from the two types of calculations in Table IV are very different. Such an amazing discrepancy can also be noticed for calculations relative to C_{60} peapods, where for a (10,10) tube, Girifalco and co-workers report an entrance energy of −3.25 eV (van der Waals calculations) to be compared to −0.4 eV for Yoon and co-workers (*ab initio* structure optimization techniques).[29] Dispersion forces are difficult to calculate and comparison with experiments is essential. For van der Waals interactions, the critical diameter Φ_{LS} between lying and standing chains, corresponding to the intersection between the energy curves E_{tot} for lying and standing molecules, is estimated to about 1.44 nm. For TEES calculations, one can deduce from Table IV that it is located above 1.44 nm (between 1.44 nm and 1.51 nm). The van der Waals model thus gives a value of Φ_{LS} closer to experiment (where it is determined to be of about 1.42 nm) than TEES calculations.

TABLE III. Distances between standing and lying C_{70} molecules from total-energy electronic-structure (TEES) and van der Waals (vdW) calculations.

	TEES	vdW
Standing	0.99 nm	1.01 nm
Lying	1.11 nm	1.13 nm

In summary, on the basis of the present data concerning C_{70} peapods, van der Waals calculations appear more reliable as far as the orientation of the molecules is concerned but the distances between molecules are better estimated using TEES calculations. One may also note that Khlobystov and co-workers briefly present density-functional based tight-binding calculations in Ref. 8 and that they obtained the lying orientation in (10,10) nanotubes ($\Phi_T=1.37$ nm) and the standing one in (11,11) nanotubes ($\Phi_T=1.51$ nm), in agreement with our results and those of Okada and co-workers.

At the end of this paper, some of the hypotheses made should be discussed in more details. First, we only considered the standing and lying orientations, while intermediate orientations may also have been considered. Second, the molecules were assumed to be located along the central axis of the nanotube while off-center positions have been predicted to occur when tube diameters are sufficiently large, leading to more complex arrangements than linear chains, such as zigzag chains.[20,26] We have thus developed further calculations within the van der Waals model. First, we minimized $E_{\text{tube,full}}$ as a function of the inclination θ of the molecule long axis with respect to the nanotube axis. It follows that between 1.40 and 1.44 nm in tube diameter, a single molecule inside the nanotube progressively reorients from the lying to the standing orientation (θ varies from 0 to 90°). Moreover, we found that if molecules are allowed to shift off the nanotube axis and if second-neighbor interaction between molecules are taken into account, zigzag chains form above

TABLE IV. $E_{\text{tube,full}}$ and E_{tot} from total-energy electronic structure (TEES) and van der Waals (vdW) calculations for standing and lying C_{70} molecules in nanotubes.

	Standing case				Lying case			
	$E_{\text{tube,full}}$ (eV)		E_{tot} (eV)		$E_{\text{tube,full}}$ (eV)		E_{tot} (eV)	
Φ_T	TEES	vdW	TEES	vdW	TEES	vdW	TEES	vdW
1.35	−0.47	0.09	−0.75	−0.27	−1.85	−3.70	−2.09	−3.96
1.43	−1.30	−3.14	−1.58	−3.5	−1.60	−3.37	−1.84	−3.63
1.51	−1.31	−2.96	−1.59	−3.32	−0.91	−2.72	−1.15	−2.98

Φ_T=1.5 nm. Accordingly, in molecular dynamic calculations performed by Troche and co-workers,[26] linear and zigzag C_{70} packings are found in (11,11) tubes (Φ_T=1.496 nm) and in (12,12) tubes (Φ_T=1.632 nm), respectively. As discussed for C_{60} chains by Hodak and Girifalco,[27] fullerene packing could even be more complicated because the perfect zigzag structure is probably not stable at room temperature, being stabilized via the rather weak second-neighbor interactions. It was noticed in Sec. IV B that agreement between simulations—made under the assumption that peapods contain only standing and lying molecules located on the tube axis—and experiments is correct but that it should be improved. Further developments of the present work should thus take into account off-centering and inclined configurations of the C_{70} molecules. However, we do believe that the present approach, although simplistic, allowed us to get the main features of the C_{70} peapod structure, that is the formation of linear chain of lying molecules below about 1.42 nm in nanotube diameter and of chains of standing molecules above.

VI. CONCLUSION

In conclusion, we have presented x-ray diffraction experiments performed on powders of C_{70} peapods and on reference single-walled nanotubes. The distribution of nanotube diameters in the samples can be described with a Gaussian function centered at 1.42 nm with FWHM=0.2 nm. We have developed a formalism to simulate diffraction patterns taking into account molecule orientations. It is shown that careful analysis of the diffraction patterns allows two critical tube diameters Φ_{enc} and Φ_{LS} to be determined. Below Φ_{enc} =1.32±0.02 nm, nanotubes are empty: encapsulation of C_{70} molecules is thermodynamically unfavorable. Between Φ_{enc} and Φ_{LS}=1.42±0.02 nm, molecules adopt the lying orientation, with their long axis parallel to the tube axis. The periodicity of linear chains of lying molecules is about 1.1 nm. Above Φ_{LS}=1.42±0.02 nm, molecules adopt the standing configuration, with their long axis perpendicular to that of the tube. Interfullerene distance is then ≃0.98 nm. Energy calculations have been performed within the scope of a van der Waals model. Calculated intermolecular distances are slightly overestimated but it is found that the calculated tube diameter Φ_{LS} being the diameter frontier between lying and standing orientations is correct. The simple van der Waals model appears here reliable as far as the orientation of the molecules is concerned.

ACKNOWLEDGMENTS

Vincent Pichot, Stéphan Rouzière, and Pierre-Antoine Albouy are acknowledged for their help in some of the x-ray scattering experiments. The authors are grateful to Philippe Lambin, Jean-Christophe Charlier, and Julien Cambedouzou for helpful discussions and to the French Programme ANR-PNANO for funding. Teams involved in this work belong to the International Research Consortium entitled "Science and Applications of the Nanotubes" (CNRS GdR 2756).

APPENDIX: ENERGY CALCULATIONS

Calculation of interaction energies have been done numerically. Let us report in some details the formula used.

The fullerene-fullerene energy in Eq. (18) corresponds to a double integration over the linear elements $dl_{1,\nu}=R_{\nu\perp}d\varphi_\nu$ and $dl_{2,\mu}=R_{\mu\perp}d\varphi_\mu$, on circles μ and ν on the two molecules [see Fig. 4(a) for the definition of $R_\perp$ and φ]. No simplification is made in the standing case, while in the lying case, defining $\varphi=\varphi_\nu-\varphi_\mu$, one easily shows that Eq. (18) gives

$$E_{\text{full-full}} = 2\pi \sum_{\nu,\mu=0}^{8} n_\nu n_\mu R_{\nu\perp} R_{\mu\perp} \int_0^{2\pi} \left(- \frac{A}{[R_{\nu\perp}^2 + R_{\mu\perp}^2 + (L+\xi_\mu-\xi_\nu)^2 - 2R_{\nu\perp}R_{\mu\perp}\cos(\varphi)]^3} + \frac{B}{[R_{\nu\perp}^2 + R_{\mu\perp}^2 + (L+\xi_\mu-\xi_\nu)^2 - 2R_{\nu\perp}R_{\mu\perp}\cos(\varphi)]^6} \right) d\varphi.$$

For the tube-fullerene energy in Eq. (19), integration must now be performed over three coordinates: the angle φ for a point M on circle ν of the molecule, an angle φ_T and the Z coordinate ξ for a point P on the nanotube. One obtains an expression of the form

$$MP^2 = F(\Phi_T, R_{\nu\perp}, \varphi, \varphi_\nu) + (\xi - \xi_\nu)^2$$

for a lying molecule and

$$MP^2 = G(\Phi_T, R_{\nu\perp}, \varphi, \varphi_\nu) + [\xi - R_{\nu\perp} \sin(\varphi_\nu)]^2$$

for a standing molecule. The variable ξ varies from $-\infty$ to ∞. Integration over ξ can be performed analytically using the recurrence formula

$$\int \frac{dz}{(a+z^2)^{n+1}} = \frac{z}{2na(a+z^2)^n} + \frac{2n-1}{2na} \int \frac{dz}{(a+z^2)^n}.$$

One obtains

$$E_{\text{tube-full}} = \frac{\pi \Phi_T \sigma_T}{2} \sum_{\nu=0}^{4} R_{\nu\perp} n'_\nu \int_0^{2\pi} d\varphi_\nu \times \int_0^{2\pi} d\varphi \left(-\frac{3A}{8f^{5/2}} + \frac{63B}{256f^{11/2}} \right),$$

where $f=F$ for a lying molecule and G for a standing one; $n'_0=n_0$ and $n'_\nu=2n_\nu$ for $\nu=1-4$. Numerical integration is performed over the two variables φ and φ_ν.

*Corresponding author. Electronic address: launois@lps.u-psud.fr

[1] B. W. Smith, M. Monthioux, and D. E. Luzzi, Nature (London) **396**, 323 (1998).

[2] M. Monthioux, Carbon **40**, 1809 (2002).

[3] *Carbon Nanotubes: Synthesis, Structure, Properties and Applications*, edited by M. Dresselhaus, G. Dresselhaus, and Ph. Avouris (Springer-Verlag, Berlin, 2001).

[4] *Understanding Carbon Nanotubes, From Basics to Applications*, edited by A. Loiseau, P. Launois, P. Petit, S. Roche, and J.-P. Salvetat Springer Series: Lecture Notes in Physics, Vol. 677 (Springer, New York, 2006).

[5] D. J. Hornbaker, S. J. Kahng, S. Misra, B. W. Smith, A. T. Johnson, E. T. Mele, D. E. Luzzi, and A. Yazdani, Science **295**, 828 (2002).

[6] P. Jaroenapibal, S. B. Chikkannanavar, D. E. Luzzi, and S. Evoy, J. Appl. Phys. **98**, 044301 (2005).

[7] K. Hirahara, S. Bandow, K. Suenaga, H. Kato, T. Okazaki, H. Shinohara, and S. Iijima, Phys. Rev. B **64**, 115420 (2001).

[8] A. N. Khlobystov, R. Scipioni, D. Nguyen-Manh, D. A. Britz, D. G. Pettifor, G. A. D. Briggs, S. G. Lyapin, A. Ardavan, and R. J. Nicholas, Appl. Phys. Lett. **84**, 792 (2004).

[9] L. Guan, H. Li, Z. Shi, L. You, and Z. Gu, Solid State Commun. **133**, 333 (2005).

[10] M. Otani, S. Okada, and A. Oshiyama, Phys. Rev. B **68**, 125424 (2003).

[11] S. Okada, M. Otani, and A. Oshiyama, New J. Phys. **5**, 122 (2003).

[12] H. Ulbricht, G. Moos, and T. Hertel, Phys. Rev. Lett. **90**, 095501 (2003).

[13] L. A. Girifalco, M. Hodak, and R. S. Lee, Phys. Rev. B **62**, 13104 (2000).

[14] C. Journet, W. K. Maser, P. Bernier, A. Loiseau, M. Lamy de la Chapelle, S. Lefrant, P. Deniard, R. Lee, and J. E. Fisher, Nature (London) **388**, 756 (1997).

[15] S. Rols, R. Almairac, L. Henrard, E. Anglaret, and J. L. Sauvajol, Eur. Phys. J. B **10**, 263 (1999).

[16] A. Thess, R. Lee, P. Nikolaev, H. Dai, P. Petit, J. Robert, C. Xu, Y. Lee, S. Kim, A. G. Rinzler, D. T. Colbert, G. E. Scuseria, D. Tomnek, J. E. Fischer, and R. E. Smalley, Science **273**, 483 (1996).

[17] Y. Maniwa, Y. Kumazawa, Y. Saito, H. Tou, H. Kataura, H. Ishii, S. Suzuki, Y. Achiba, A. Fujiwara, and H. Suematsu, Jpn. J. Appl. Phys., Part 2 **38**, L668 (1999).

[18] J. Cambedouzou, V. Pichot, S. Rols, P. Launois, P. Petit, R. Klement, H. Kataura, and R. Almairac, Eur. Phys. J. B **42**, 31 (2004).

[19] Y. Maniwa, H. Kataura, M. Abe, A. Fujiwara, R. Fujiwara, H. Kira, H. Tou, S. Suzuki, Y. Achiba, E. Nishibori, M. Takata, M. Sakata, and H. Suematsu, J. Phys. Soc. Jpn. **72**, 45 (2003).

[20] M. Hodak and L. A. Girifalco, Phys. Rev. B **67**, 075419 (2003).

[21] K. H. Michel, B. Verberck, and A. V. Nikolaev, Phys. Rev. Lett. **95**, 185506 (2005).

[22] K. H. Michel, B. Verberck, and A. V. Nikolaev, Eur. Phys. J. B **48**, 113 (2005).

[23] S. Ravy, P. Launois, R. Moret, and J.-P. Pouget, Z. Kristallogr. **220**, 1059 (2005).

[24] W. Zhou, K. I. Winey, J. E. Fischer, T. V. Sreekumar, S. Kumar, and H. Kataura, Appl. Phys. Lett. **84**, 2172 (2004).

[25] M. Hodak and L. A. Girifalco, Chem. Phys. Lett. **363**, 93 (2002).

[26] K. S. Troche, V. R. Coluci, S. F. Braga, D. D. Chinellato, F. Sato, S. B. Legoas, R. Rurali, and D. S. Galvao, Nano Lett. **5**, 349 (2005).

[27] M. Hodak and L. A. Girifalco, Phys. Rev. B **68**, 085405 (2003).

[28] P. Launois, S. Ravy, and R. Moret, Int. J. Mod. Phys. B **13**, 253 (1999).

[29] M. Yoon, S. Berber, and D. Tománek, Phys. Rev. B **71**, 155406 (2005).